Heat Transport by Currents Across 25°N Latitude in the Atlantic Ocean

Abstract. *The heat transported by currents across 25°N in the Atlantic Ocean is estimated from oceanographic measurements to be* 1.1×10^{15} *watts northward. This figure agrees, within estimated error, with the value obtained from charts of energy exchange between ocean and atmosphere but is smaller by a factor of 2 than the recent value derived from satellite radiation measurements.*

Recent studies of satellite radiation measurements combined with estimates of atmospheric heat transport have yielded values for oceanic heat transport in subtropical regions that are approximately twice as large as those estimated from charts of energy exchange between ocean and atmosphere (*1*). Because studies of oceanic heat transport based on oceanographic measurements have either avoided regions with western boundary currents such as the Gulf Stream or have had great difficulty determining even the direction of ocean heat transport across latitudes with western boundary currents (*2*), no direct estimates of heat transport by currents have been made in the subtropical Atlantic Ocean where indirect methods suggest oceanic heat transport is largest. To provide a direct estimate for comparison with indirect estimates, we compute here the heat transport by currents across 25°N in the Atlantic Ocean where the required oceanographic measurements have been made.

Detailed current and temperature measurements in the Gulf Stream as it flows through the Florida Straits (*3*) and a transoceanic hydrographic section from the Bahamas to Africa (*4*) have been made. From these measurements and values of wind stress (*5*), we estimate the heat transport by ocean currents across 25°N. To estimate oceanic heat transport, it is necessary first to balance the mass or volume transport and then to consider the temperatures of northward-flowing water and returning southward-flowing water. The transport multiplied by the difference in temperature then yields the heat transport.

Analysis of current and temperature measurements in the Florida Straits has shown an annual cycle in volume transport of the Gulf Stream of amplitude $4.1 \times 10^{6}\ \mathrm{m^3\ sec^{-1}}$ about a mean transport of $29.5 \times 10^{6}\ \mathrm{m^3\ sec^{-1}}$ and has suggested a large difference between summer and winter heat transports (*3*). The difference in heat transports, however, is due to the variability in volume transport and not to a change in temperature of the flow (*6*). In fact, dividing winter heat transport by winter volume transport and summer heat transport by summer volume transport (*7*) shows that the average temperature of flow through the Florida Straits varies only by 0.5°C about 18.8°C. Hence, we estimate the average temperature for the northward flow of $29.5 \times 10^{6}\ \mathrm{m^3\ sec^{-1}}$ through the Florida Straits to be 18.8°C. For comparison with estimates from the transoceanic section, we divide the contribution of this flow into three parts: (i) a barotropic (or depth-averaged) geostrophic flow of $29.4 \times 10^{6}\ \mathrm{m^3\ sec^{-1}}$ at an area-averaged temperature of 16°C; (ii) a northward wind-driven transport of $0.1 \times 10^{6}\ \mathrm{m^3\ sec^{-1}}$ in the near-surface layer at an average temperature of 26.4°C; and (iii) a baroclinic heat transport, in which warmer water flows northward relative to the barotropic flow and colder water flows relatively southward with no net baroclinic volume transport, of 0.33×10^{15} W northward (Table 1).

Because the Atlantic north of 25°N is nearly a closed basin with only $1 \times 10^{6}\ \mathrm{m^3\ sec^{-1}}$ of water entering from the Arctic (*8*), the northward transport through the Florida Straits must return southward across the section from the Bahamas to Africa. We assume that this return flow is in geostrophic balance except for wind-driven flow in the near-surface waters. From values of zonal wind stress τ^x (*5*), the northward wind-driven transport across this section is $5.0 \times 10^{6}\ \mathrm{m^3\ sec^{-1}}$. Distributing this transport in the upper 50 m and calculating a weighted average of surface and 50-m temperatures, we estimate that this wind-driven transport occurs at an average temperature of 26.0°C. Thus, across the section between the Bahamas and Africa there must be a southward, geostrophic transport of $34.5 \times 10^{6}\ \mathrm{m^3\ sec^{-1}}$, of which $29.4 \times 10^{6}\ \mathrm{m^3\ sec^{-1}}$ balances the northward geostrophic flow through the Florida Straits and $5.1 \times 10^{6}\ \mathrm{m^3\ sec^{-1}}$ balances the wind-driven flow.

To determine the distribution of the southward return flow and its average temperature, northward currents are calculated geostrophically for each adjacent pair of stations in the transoceanic hydrographic section at 24.5°N (*4*). The reference level is chosen so that the vertically averaged baroclinic current is zero for each pair. Hence the total geostrophic northward velocity, v, for each pair is the sum of a reference level velocity, v_r, which is constant over depth and a baroclinic velocity profile, $v'(z)$, with zero depth-averaged value

$$v = v'(z) + v_r$$

Likewise, the average potential temperature, θ, for each adjacent station pair is the sum of the depth-averaged potential temperature, θ_r, and a baroclinic potential temperature profile, $\theta'(z)$ with zero depth-averaged value

$$\theta = \theta'(z) + \theta_r$$

The baroclinic heat transport,

$$\iint dx\, dz\, \rho\, C_p\, v'\theta'$$

where x is eastward and z is upward distance, ρ is the seawater density, and C_p is the specific heat capacity of seawater, is estimated in a straightforward manner to be 0.93×10^{15} W southward; that is, the baroclinic flow is such that warmer

Table 1. Northward heat transport by currents across 25°N in the Atlantic Ocean. Positive values denote northward heat transport or northward volume transport.

Component	Barotropic flow	Wind-driven flow	Baroclinic heat transport (W)	Volume transport and average temperature
Florida Straits	$+29.4 \times 10^{6}\ \mathrm{m^3\ sec^{-1}}$ at 16°C	$+0.1 \times 10^{6}\ \mathrm{m^3\ sec^{-1}}$ at 26.4°C	$+0.33 \times 10^{15}$	$+29.5 \times 10^{6}\ \mathrm{m^3\ sec^{-1}}$ at 18.8°C
Sections from the Bahamas to Africa		$+5.0 \times 10^{6}\ \mathrm{m^3\ sec^{-1}}$ at 26.0°C	-0.93×10^{15}	$29.5 \times 10^{6}\ \mathrm{m^3\ sec^{-1}}$ at 9.7°C
Compensating return flow across the section from the Bahamas to Africa	$-29.4 \times 10^{6}\ \mathrm{m^3\ sec^{-1}}$ at 5.4°C	$-5.1 \times 10^{6}\ \mathrm{m^3\ sec^{-1}}$ at 5.4°C		
Heat transport by ocean currents	$+1.27 \times 10^{15}$ W	$+0.43 \times 10^{15}$ W	-0.60×10^{15}	$+1.10 \times 10^{15}$ W

0036-8075/80/0222-0884$00.50/0 Copyright © 1980 AAAS

water flows southward relative to the depth-averaged current while colder water flows relatively northward.

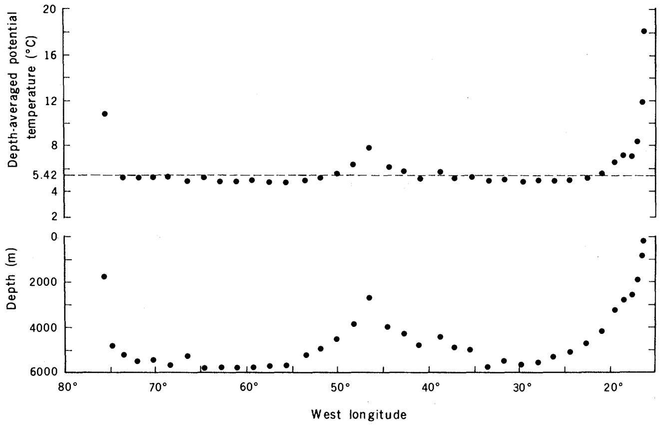

Fig. 1. Depth-averaged potential temperature (top) and average depth (bottom) versus zonal distance across 25°N in the Atlantic from the Bahamas on the west to Africa on the east.

Although the distribution of reference level velocities across the section is unknown, the vertical and zonal integral of v_r across the section must equal the southward geostrophic transport of 34.5×10^6 m^3 sec^{-1}. Since θ_r for each station pair is nearly constant across most of the section (Fig. 1), we assign its zonally averaged value of 5.4°C to the barotropic southward return flow of 34.5×10^6 m^3 sec^{-1}. The value of θ_r varies significantly from its zonal mean only in shallow regions along the continental slopes near the Bahamas and Africa and over the Mid-Atlantic Ridge. Although there are no current measurements from which to determine barotropic currents in these shallow regions, we used an inverse method solution (*9*) to estimate a northward transport of 2.1×10^6 m^3 sec^{-1} along the Bahamian continental slope, direct current measurements at 21.7°N (*10*) to estimate a southward transport of 1.1×10^6 m^3 sec^{-1} along the African continental slope, and direct current measurements at 27.5°N (*11*) to estimate a northward transport of 8.7×10^6 m^3 sec^{-1} over the Mid-Atlantic Ridge. If we had included these transports and their average temperatures, the heat transport by barotropic flow in Table 1 would have increased by 0.09×10^{15} W northward, or less than 7 percent.

The heat transport by currents across 25°N in the Atlantic Ocean then is estimated from the sum of three components (Table 1). The barotropic heat transport due to 29.4×10^6 m^3 sec^{-1} of 16°C water flowing northward through the Florida Straits and returning southward across the section from the Bahamas to Africa at 5.4°C is 1.27×10^{15} W northward. We associate this component with the large-scale, anticyclonic horizontal circulation in the North Atlantic. The heat transport due to wind driving 5.1×10^6 m^3 sec^{-1} of 26°C water northward with 5.4°C water returning southward is 0.43×10^{15} W northward. We associate this component with the vertical-meridional, wind-driven Ekman circulation. The large-scale horizontal circulation then transports approximately three times as much heat northward as the Ekman circulation. The baroclinic heat transport due to warmer water flowing southward relative to the barotropic current with colder water flowing relatively northward is 0.60×10^{15} W southward. We associate this component with the vertical-meridional, geostrophic circulation. The net heat transport by currents across 25°N in the Atlantic Ocean then equals the sum of the three components which is 1.10×10^{15} W northward.

Because we consider this estimate to be one of yearly averaged oceanic heat transport, we have used annual averages of Florida Straits transport and of zonal wind stress. However, only the single transoceanic hydrographic section, made during October 1957, is available for estimating baroclinic heat transport. The largest error in our estimate of oceanic heat transport is due to uncertainty in using a single section to estimate yearly averaged baroclinic heat transport. The baroclinic heat transport from this section of -0.93×10^{15} W (Table 1) can be divided into a contribution due to zonally averaged baroclinic velocities and temperatures of -0.64×10^{15} W and an eddy contribution due to deviations of baroclinic velocities and temperatures from their zonal averages of -0.29×10^{15} W. Because the section is so wide, traditional error analysis for hydrographic measurements (*12*) suggests that the contribution due to zonally averaged velocities and temperatures has less than 10 percent error. Because the standard error of eddy contributions for the 37 station pairs is as large as the mean eddy contribution, the error in eddy contribution is taken to be $\pm 0.29 \times 10^{15}$ W. Since this is the largest error by far, we consider the error in our estimate of oceanic heat transport across 25°N to be $\pm 0.29 \times 10^{15}$ W.

Two independent, indirect methods are used for estimating oceanic heat transport. The traditional indirect method is to integrate the exchange of energy between ocean and atmosphere determined from bulk equations for all regions poleward of the chosen latitude. The net energy lost by the ocean then must have been carried poleward by ocean currents across the chosen latitude (*13*). From the most modern tables of energy exchange for the Atlantic (*14*), we estimate a net loss of energy by the ocean to the atmosphere north of 25°N of 1.11×10^{15} W. In the second indirect method satellite radiation measurements are used to estimate combined oceanic and atmospheric heat transport and then atmospheric heat transport is subtracted to derive a residual value for oceanic heat transport. The most recent estimate of oceanic heat transport for the combined world oceans at 25°N by this method is 2.5×10^{15} W (*1*). Using a result from energy exchange analysis that the Atlantic is responsible for more than 70 percent of the total oceanic heat transport at this latitude (*15*), we estimate that this second indirect method yields a value for oceanic heat transport across 25°N in the Atlantic of 1.8×10^{15} W.

Thus, the direct estimate of heat transport by ocean currents determined here agrees, within estimated error, with the indirect estimate based on energy exchange between ocean and atmosphere but is smaller by a factor of almost 2 than the indirect estimate based on satellite radiation measurements. The agreement of the direct estimate with the indirect estimate based on energy exchange presents strong evidence that the northward heat transport by ocean currents across 25°N in the Atlantic is $1.1 \pm 0.3 \times 10^{15}$ W.

HARRY L. BRYDEN
MINDY M. HALL
Department of Physical Oceanography,
Woods Hole Oceanographic Institution,
Woods Hole, Massachusetts 02543

References and Notes

1. A. H. Oort and T. H. Vonder Haar, *J. Phys. Oceanogr.* **6**, 781 (1976); T. H. Vonder Haar and A. H. Oort, *ibid.* **3**, 169 (1973).
2. A. F. Bennett, *ibid.* **8**, 785 (1978); K. Bryan, *J. Geophys. Res.* **67**, 3403 (1962).
3. P. P. Niiler and W. S. Richardson, *J. Mar. Res.* **31**, 144 (1973).
4. F. C. Fuglister, *Atlantic Ocean Atlas* (Woods Hole Oceanographic Institution, Woods Hole, Mass., 1960).
5. A. Leetmaa and A. F. Bunker, *J. Mar. Res.* **36**, 311 (1978).
6. R. B. Montgomery, *ibid.* **32**, 533 (1974); P. P. Niiler and W. S. Richardson, *ibid.*, p. 534.
7. We determined winter and summer heat transports by planimeter from figure 14 and winter

and summer volume transports from figure 2 of (3).

8. L. V. Worthington, *On the North Atlantic Circulation* (Johns Hopkins Press, Baltimore, 1976), p. 34.
9. D. H. Roemmich, "The application of inverse methods to problems in ocean circulation," thesis, Massachusetts Institute of Technology-Woods Hole Oceanographic Institution Joint Program (1979).
10. D. Halpern, J. R. Holbrook, R. M. Reynolds, "A compilation of wind, current, and temperature measurements: near Spanish Sahara during March and April 1974" (Reference M75-103, Department of Oceanography, University of Washington, Seattle, 1975); R. D. Pillsbury, J. S. Bottero, R. E. Still, E. Mittelstaedt, "A compilation of observations from moored current meters: wind, currents, and temperature off northwest Africa along 21°40′N during JOINT-I, February-April 1974" (Reference 74-20, School of Oceanography, Oregon State University, Corvallis, 1974).
11. L. Fu and C. Wunsch, *POLYMODE News* (Woods Hole Oceanographic Institution, unpublished document) **60**, 1 (1979).
12. L. M. Fomin, *The Dynamic Method in Oceanography* (Elsevier, New York, 1964).
13. W. D. Sellers, *Physical Climatology* (Univ. of Chicago Press, Chicago, 1965).
14. A. F. Bunker, *Mon. Weather Rev.* **104**, 1122 (1976).
15. H. U. Sverdrup, *Hand. Phys.* **48**, 608 (1957).
16. Support for this research was provided by a summer fellowship from C. S. Payson and by grants OCE 77-19403 and OCE 77-22887 from the Office for the International Decade of Ocean Exploration of the National Science Foundation. R. deSzoeke suggested searching for a section where depth-averaged potential temperature has small variation. We thank K. Bryan, A. Gill, P. Rhines, and H. Stommel for stimulating discussions and R. Montgomery, P. Niiler, B. Warren, and V. Worthington for helpful criticism. A. Bunker's help in locating values of wind stress and of energy exchange between ocean and atmosphere and his encouragement for this study were invaluable. Woods Hole Oceanographic Institution contribution 4433 and POLYMODE contribution 124.

17 September 1979; revised 27 November 1979

Free-Radical Oxidants in Natural Waters

Abstract. *Photooxidation of cumene (isopropylbenzene) and pyridine in dilute solution in natural waters gives products characteristic of reactions with alkylperoxy* ($RO_2\cdot$) *and hydroxyl* ($HO\cdot$) *radicals. On the basis of the rates of formation of the products, the average concentrations of* $RO_2\cdot$ *and* $HO\cdot$ *are estimated to be about* 10^{-9} *and* 10^{-17} *mole per liter, respectively. The concentration of* $RO_2\cdot$ *is large enough that, for some classes of reactive chemicals, oxidation can be an important process in natural waters.*

An amazing variety of synthetic organic chemicals are found in the waterways of the United States, many in significant concentrations (*1*). Their fates are largely unknown, although dilution, biodegradation, volatilization, hydrolysis, and photooxidation processes have all been implicated in their loss (*2*). Several investigators have reported evidence of free-radical oxidations of chemicals exposed to sunlight (or light of wavelength above 300 nm) in natural waters but not in pure water (*2*). The implication is that when the natural organics present in many water bodies undergo photolysis, they generate free radicals such as alkylperoxy ($RO_2\cdot$) or hydroxyl ($HO\cdot$) and other oxidants such as singlet oxygen ($^1O_2$) (*3*) and that these oxidants contribute to the transformation of some synthetic chemicals in water. We have investigated the importance of free radicals as oxidants for organic chemicals in a variety of natural waters, using cumene (isopropylbenzene) and pyridine (C_5H_5N) to probe quantitatively for $RO_2\cdot$ and $HO\cdot$.

In our laboratory experiments only one kind of radical was generated in pure water; we used azo-bis(2-carbomethoxypropane) (MAB) as a thermal source of $RO_2\cdot$ (*4*) and $10^{-3}M$ H_2O_2 in water, photolyzed with > 290-nm light, as a source of $HO\cdot$ (*4a*). All the significant oxidation products from each kind of experiment were measured and identified.

Table 1 summarizes the experimental results and shows that cumene (CuH) at $10^{-4}M$ in pure water oxidizes readily in the presence of $RO_2\cdot$ and O_2 to give only products from side-chain oxidation: cumyl hydroperoxide (CuOOH), cumyl alcohol (CuOH), and acetophenone ($C_6H_5COCH_3$). However, $HO\cdot$ oxidizes CuH in water to form both side-chain and ring oxidation products, including 2- and 4-isopropylphenols in a 30:70 ratio (*5*). The following reactions summarize the radical oxidation of CuH:

$$RO_2\cdot + CuH \rightarrow RO_2H + Cu\cdot$$

$$Cu\cdot + O_2 \rightarrow CuO_2\cdot$$

$$CuO_2\cdot + CuH \rightarrow CuO_2H + Cu\cdot$$

$$CuO_2\cdot + RO_2\cdot \rightarrow CuO\cdot + RO\cdot + O_2$$

$$CuO\cdot \rightarrow C_6H_5COCH_3 + CH_3\cdot$$

$$CH_3\cdot + O_2 + CuO_2\cdot \rightarrow CH_2O + CuOH + O_2 \text{ (two steps)}$$

$$HO\cdot + CuH \rightarrow H_2O + Cu\cdot$$

$$HO\cdot + O_2 + CuH \rightarrow HOC_6H_4\text{-}i\text{-}C_3H_7 + HO_2\cdot \text{ (two steps)}$$

where $HOC_6H_4\text{-}i\text{-}C_3H_7$ is hydroxyisopropylbenzene.

These experiments provide the basis for interpreting results from experiments with CuH dissolved in natural waters and exposed to light. Photolyses of CuH dissolved in filter-sterilized natural waters and then exposed to either sunlight or to a xenon lamp (*6*) gave mixtures of the same side-chain and ring oxidation products found in radical-initiated reactions (Table 1). Table 2 summarizes these results. In all cases except for pure water, the proportions of side-chain and ring oxidation products were such that participation by both $RO_2\cdot$ and $HO\cdot$ is required to account for the results.

The ratio of products from side-chain and ring oxidation (*S*/*R*) evidently does not vary widely either in the same water source sampled at different times or in difference sources; the Aucilla River, a highly eutrophic river in northern Florida, showed somewhat greater activity than Coyote Creek or Boronda Lake and also exhibits much higher absorptivity in the solar region. The different relative proportions of oxidation products of $RO_2\cdot$ or $HO\cdot$ found may be due to different secondary reactions as well as different spectral, photochemical, and chemical properties of the waters (*7*).

We measured the products and the *S*/*R* ratio from CuH at several times in one experiment with photolyzing Aucilla River water containing $1 \times 10^{-4}M$ CuH. No significant change in *S*/*R* was found over a 144-hour period (measured at 24, 72, and 144 hours); this result indicates that phenols did not arise from the photolysis of initially formed CuOOH.

Table 1. Distribution of oxidation products from CuH oxidized in pure water at 50°C (concentrations are in $M \times 10^{-6}$).

Radical (source)	$[CuH]_0$	[Products]*		
		Side chain† (*S*)	Ring‡ (*R*)	*S*/*R*
$RO_2\cdot$ (MAB)§	303	9.27 ± 0.5	< 0.02	> 500
$RO_2\cdot$ (MAB)‖	245	7.65 ± 0.4	< 0.01	> 800
$RO_2\cdot$ (MAB)¶	23	3.44 ± 0.2	< 0.01	> 300
$HO\cdot$ (H_2O_2)#	~ 220	2.85 ± 0.2	6.68 ± 0.4	0.43

*Values averaged from three or more analyses; we analyzed the products by using an hplc C_{18} μ-Bondapak column (4 mm by 30 cm) and gradient elution of an acetonitrile-water mixture from 10 to 100 percent in acetonitrile in 30 minutes with 2 ml min^{-1} throughput. An ultraviolet detector set at 254 nm was used to measure products by comparison with peak areas for known mixtures. †Sum of CuOH, CuOOH, and $C_6H_5COCH_3$. ‡Sum of 2- and 4-hydroxyisopropylbenzenes; identity of these products was confirmed by gas chromatography-mass spectroscopy. §$[MAB]_0 = 1.45 \times 10^{-4}M$; 24-hour experiment. ‖$[MAB]_0 = 1.00 \times 10^{-4}M$; 24-hour experiment. ¶$[MAB]_0 = 1.03 \times 10^{-4}M$; 72 hour experiment. #$[H_2O_2]_0 = 1.0 \times 10^{-3}M$; experiments were carried out at 30°C with a xenon light source (*6*).